Published June 24, 2002

Chemokine Requirements for B Cell Entry to Lymph Nodes and Peyer's Patches

Takaharu Okada,[1] Vu N. Ngo,[1] Eric H. Ekland,[1] Reinhold Förster,[2] Martin Lipp,[3] Dan R. Littman,[4] and Jason G. Cyster[1]

[1]*Howard Hughes Medical Institute and Department of Microbiology and Immunology, University of California San Francisco, San Francisco, CA 94143*
[2]*Institute of Immunology, Hannover Medical School, 30625 Hannover, Germany*
[3]*Molecular Tumorgenetics and Immunogenetics, Max-Delbrück-Center for Molecular Medicine, 13092 Berlin, Germany*
[4]*Howard Hughes Medical Institute, Skirball Institute of Biomolecular Medicine, New York University Medical Center, New York, NY 10016*

Abstract

B cell entry to lymph nodes and Peyer's patches depends on chemokine receptor signaling, but the principal chemokine involved has not been defined. Here we show that the homing of $CXCR4^{-/-}$ B cells is suppressed in CCL19 (ELC)- and CCL21 (SLC)-deficient paucity of lymph node T cells mice, but not in wild-type mice. We also find that CXCR4 can contribute to T cell homing. Using intravital microscopy, we find that B cell adhesion to high endothelial venules (HEVs) is disrupted when CCR7 and CXCR4 are predesensitized. In Peyer's patches, B cell entry is dependent on CXCR5 in addition to CCR7/CXCR4. CXCL12 (SDF1) is displayed broadly on HEVs, whereas CXCL13 (BLC) is found selectively on Peyer's patch follicular HEVs. These findings establish the principal chemokine and chemokine receptor requirements for B cell entry to lymph nodes and Peyer's patches.

Key words: chemokine • high endothelial venule • adhesion • lymphoid organ • B cell

Introduction

Lymphocyte passage from blood into lymph nodes and Peyer's patches is a multistep process (1, 2). First, lymphocytes are captured and roll on high endothelial venules (HEVs)* via adhesive interaction between the selectins on lymphocytes and their counterreceptors on HEVs. This selectin-supported rolling is followed by triggering events signaled through Gi protein–coupled receptors that induce integrin-dependent firm adhesion. Once firm adhesion has been achieved, the lymphocytes proceed through an additional series of steps that lead to migration across the endothelium and movement into the lymphoid tissue.

The critical involvement of Gi protein–coupled signaling in T and B lymphocyte homing was established through the discovery of a strong inhibitory effect of pertussis toxin on lymphocyte homing (3–6). This finding implicated chemokines and chemokine receptors in T and B lymphocyte entry to lymphoid tissues, as all chemokine receptors couple to pertussis toxin–sensitive G proteins. Circulating B and T lymphocytes express multiple chemokine receptors including CCR7, the receptor for CCL19 (ELC) and CCL21 (SLC), CXCR4, the receptor for CXCL12 (SDF1), and in the case of B cells, CXCR5, the receptor for CXCL13 (BLC). CCL21 was found to be expressed at high levels by HEVs (7) and more recently, CCL19 has been observed on HEVs (8). In flow chamber studies, both CCL21 and CCL19 could promote firm adhesion of rolling lymphocytes (9, 10). A critical role for CCR7 and CCL19/CCL21 in T cell homing has been established from genetic studies. Mice homozygous for a spontaneous mutation, paucity of lymph node T cells (*plt*), lack the CCL19 gene and the gene for lymphoid tissue, CCL21 (CCL21-ser; references 11–14). Transfer studies have established that *plt/plt* mice are poorly able to support the

The online version of this article contains supplemental material.

Address correspondence to Jason G. Cyster, Department of Microbiology and Immunology, University of California San Francisco, 513 Parnassus Avenue, San Francisco, CA 94143. Phone: 415-502-6427; Fax: 415-502-8424; E-mail: cyster@itsa.ucsf.edu

**Abbreviations used in this paper:* AP, alkaline phosphatase; B6, C57BL/6 mice; CFSE, 5- and 6-carboxyfluorescein diacetate succinimidyl ester; FBS, fetal bovine serum; HEV, high endothelial venule; HRP, horseradish peroxidase; ICAM1, intercellular adhesion molecule 1; MAdCAM, mucosal addressin cell adhesion molecule; plt, paucity of lymph node T cells; PNAd, peripheral node addressin; TRITC, tetramethylrhodamine-5- and 6-isothiocyanate.

J. Exp. Med. © The Rockefeller University Press • 0022-1007/2002/07/65/11 $5.00
Volume 196, Number 1, July 1, 2002 65–75
http://www.jem.org/cgi/doi/10.1084/jem.20020201

Published June 24, 2002

firm adhesion of T cells to HEVs (15, 16). A second CCL21 gene that differs from CCL21-ser in a single codon, CCL21-leu, is retained in *plt/plt* mice and expressed by lymphatic vessels outside lymphoid tissues (12, 14). Consistent with the findings in *plt/plt* mice, T cells lacking CCR7 are markedly suppressed in their ability to enter wild-type lymph nodes and Peyer's patches (17). Therefore, CCL19/CCL21 and the receptor CCR7 play an important role in the multistep process of T lymphocyte entry to lymph nodes and Peyer's patches.

Despite the significant advances in our understanding of the chemokine requirements for T cell homing across HEVs, the chemokine(s) involved in B cell homing are not well established. Although transferred CCR7-deficient B cells showed diminished accumulation in lymph nodes and Peyer's patches compared with wild-type B cells, no such effect was seen on B cell homing to the lymph nodes of *plt* mice (17, 18). Furthermore, the transition from rolling to firm adhesion of B cells in Peyer's patch HEVs was not affected by using *plt* mice as recipients, nor by predesensitizing CCR7 on donor B cells (16). Interestingly, CCR7 and its ligands also do not fully account for T cell homing to lymph nodes and Peyer's patches, as a small number of CCR7-deficient T cells were observed to enter these tissues in short-term transfer experiments (17).

No chemokines other than CCL19/CCL21 have been directly established to function in lymphocyte homing to lymph nodes and Peyer's patches. CXCL12 and its receptor, CXCR4, function in B cell development by promoting the retention of B cell precursors in bone marrow (19 and references therein). However, in the periphery, CXCR4-deficient lymphocytes were found to efficiently repopulate secondary lymphoid organs (19). In addition, although CXCL12 promoted lymphocyte adhesion in flow chamber studies (9), the desensitization of CXCR4 did not affect the transition from rolling to sticking of B or T cells in Peyer's patch HEVs (16). Studies of CXCL13 and CXCR5 have shown that naive B cells and a subset of activated and memory T cells localize in a CXCR5-dependent manner in the lymphoid follicles where CXCL13 is produced (20, 21). However, so far there has not been any evidence that these molecules take part in the mechanism of lymphocyte entry into lymphoid organs.

Here we find that the combined blockade of the chemokine signals through CXCR4 and CCR7 strongly diminishes the homing of B cells to lymph nodes and Peyer's patches. CXCL12 mRNA was found in cells adjacent to HEVs, and protein could be detected on the HEV lumen. Intravital microscopy with chemokine-desensitized cells revealed that CXCR4 and CCR7 are used for the transition of B cells from rolling to firm adhesion on HEVs. Furthermore, we show that CXCL13 and CXCR5 play an important role in B cell homing to Peyer's patches.

Materials and Methods

Mice and Fetal Liver Chimeras. C57BL/6 (B6) mice were purchased from Jackson ImmunoResearch Laboratories, and B6-Ly5^a, BALB/c, and B6 mice with jugular vein catheters were purchased from Charles River Laboratories. Mice with *plt* mutation on BALB/c background (BALB/c-*plt/plt*; reference 18) were crossed with B6 six times and intercrossed to generate *plt/plt* homozygous mice (termed B6-plt/plt). CXCR5$^{+/-}$, CXCR5$^{-/-}$, and BLC$^{-/-}$ mice were on a mixed B6 and 129 background and were screened as previously described (20, 21). To make CXCR4$^{+/+}$ or CXCR4$^{-/-}$ chimeras, B6-Ly5^a mice that had been lethally irradiated were reconstituted with CXCR4$^{+/+}$ or CXCR4$^{-/-}$ fetal liver cells as previously described (22). The CXCR4 mutation was generated on the 129 background and had been backcrossed six generations to B6. To provide CCR7$^{-/-}$ cells for adoptive transfer, bone marrow from CCR7$^{-/-}$ mice on a mixed B6 and 129 background (17), and that in some cases also carried Ig^{HEL}-transgenes (23), was used to reconstitute lethally irradiated B6 mice, as previously described (24). After 5–6 wk of reconstitution, spleen cells from the CCR7$^{-/-}$ chimeric animals were used for adoptive transfers. No differences were observed in the homing of non- or Ig-transgenic CCR7$^{-/-}$ B cells.

Adoptive Transfer. Splenocytes from CXCR4$^{+/+}$ or CXCR4$^{-/-}$ chimeras, and CXCR5$^{+/-}$, CXCR5$^{-/-}$, or CXCL13$^{-/-}$ mice were resuspended in DMEM with 1% fetal bovine serum (FBS) and labeled with 0.5 μM 5- and 6-carboxyfluorescein diacetate succinimidyl ester (CFSE; Molecular Probes) for 10 min at 37°C, washed once in DMEM with 10% FBS, and once in DMEM with 1% FBS. After mixing with splenocytes from B6-Ly5^a mice at a 1:1 ratio, cells were injected into the lateral tail vein of two ~5-mo-old B6 or age-matched B6-*plt/plt* mice (3×10^7 cells in 0.3 ml per mouse). BALB/c splenocytes were CFSE labeled and transferred to BALB/c or BALB/c-*plt/plt* recipients. Lymphoid organ cells of recipient mice were harvested 90 min after transfer, counted, and subject to flow cytometric analyses. For desensitization experiments, spleen and lymph node cells from B6 mice were labeled with CFSE as described above, and incubated with PBS, 10 μg/ml mouse CCL19 (R&D Systems), 10 μg/ml human CXCL12 (Gryphon Laboratories), or combined CCL19 and CXCL12 (10 μg/ml each) for 45 min at 37°C. Cells were transferred into 6-wk-old B6 mice (3×10^7 cells in 0.3 ml per mouse), and lymphoid organ cells of recipient mice were harvested 20 min after transfer, counted, and subjected to flow cytometric analyses. To normalize for the differences in the number of cells injected into each recipient, transfer data were plotted as the number of cells of each type recovered in each recipient per 10^6 cells of the type intravenously transferred into the recipient.

Flow Cytometry. Lymphoid organ cells from recipient mice in adoptive transfer experiments were stained for flow cytometry. The following antibodies were used for surface staining: rat anti–B220-Tricolor, rat anti–CD4-PE, rat anti–CD8a-PE (Caltag), hamster anti–CD3e-biotin, rat anti–CD4-PerCP, rat anti–CD8a-PerCP, and mouse anti–CD45.1 (Ly5^a)-PE (BD PharMingen). Hamster anti–CD3e-biotin was detected using streptavidin-allophycocyanin (Molecular Probes). Stained cells were analyzed on a FACSCaliber® (Becton Dickinson).

Immunohistochemistry and In Situ Hybridization. 7–8-μm cryostat sections of lymph nodes and Peyer's patches of 6–10-wk-old B6 mice were fixed in acetone and stained as previously described (21) with the following antibodies: goat anti–CXCL12 (Santa Cruz Biotechnology, Inc.), goat anti–mouse CCL21, or goat anti–mouse CXCL13 (R&D Systems); rat IgM anti–peripheral node addressin (PNAd) or rat anti–mucosal addressin cell adhesion molecule (MAdCAM; BD PharMingen); and rat anti–

B220-biotin (Caltag). Goat anti–CXCL12 antibody, after incubation with or without CXCL12 blocking peptide (62.5 μg/1 mg antibody; Santa Cruz Biotechnology, Inc.) for 1 h on ice, was centrifuged at 13,000 rpm for 1 min, and the supernatant was used for staining. Goat antibodies were detected using biotinylated donkey anti–goat IgG antibody (Jackson ImmunoResearch Laboratories) and Vectastain® ABC-alkaline phosphatase (AP) kit (Vector Laboratories). Rat IgM anti–PNAd antibody was detected using horseradish peroxidase (HRP)-conjugated mouse anti–rat IgM antibody (Southern Biotechnology Associates, Inc.). Rat anti–MAdCAM antibody was detected using HRP-conjugated donkey anti–rat IgG antibody (Jackson ImmunoResearch Laboratories). Rat anti–B220-biotin was detected using AP-conjugated streptavidin (Jackson ImmunoResearch Laboratories). AP and HRP were detected as previously described (21). In situ hybridization was performed as previously described (22, 25).

Intravital and Whole Mount Microscopy. B6 mice with jugular vein catheters were anesthetized by intraperitoneal injection of 10 ml/kg saline containing 1 mg/ml xylazine and 5 mg/ml ketamine. Superficial inguinal lymph nodes were prepared for intravital microscopy as previously described (26). Mice were transferred to a fluorescence microscope (E800; Nikon) that was equipped with an intensified CCD camera (ICCD-350F; Video Scope International) connected to a Mini DV recorder (GV-D900; Sony). Donor B cells were purified from the spleen and lymph node cells of B6 mice by staining non–B cells with anti–CD43-biotin (BD PharMingen), and depleted using streptavidin MACS® beads and a MACS® (Miltenyi Biotec). Purity, as determined by B220 and CD3 staining, was >95% B cells and T cell contamination was <0.5%. 3×10^7/ml purified B cells were labeled with 2 or 20 μM CFSE and incubated with PBS or combined CCL19 and CXCL12 (10 μg/ml each) for 45 min at 37°C. 1.5×10^7 cells in 0.15 ml, which had been labeled with 2 μM CFSE and incubated with PBS or chemokines, were injected into mice via jugular vein catheters, and movements of transferred cells in HEV branches (order II through IV venules according to designations by von Andrian [26]) were recorded for 15 min after injection. After turning down the camera gain so that the fluorescence of cells labeled with 2 μM CFSE was hardly detected, 1.5×10^7 cells in 0.15 ml, which had been labeled with 20 μM CFSE and incubated with PBS or chemokines, were injected, and cell movements in identical HEV branches were recorded for another 15 min. From the recorded images, the numbers of freely flowing cells, rolling cells, and cells arrested on vessels were counted. For whole mount microscopy, purified B cells were labeled with either 20 μM CFSE or 20 μM tetramethylrhodamine-5- and 6-isothiocyanate (TRITC; Molecular Probes, Inc.) using the same procedure as previously described, and transferred to wild-type recipients. After 20 min, Peyer's patches were isolated, placed in Fluoromount-G (Southern Biotechnology Associates, Inc.), and examined by fluorescence microscopy.

Online Supplemental Material. QuickTime™ videos showing characteristic scenes from intravital microscopy experiments of PBS-treated B cells and CCL19- plus CXCL12-desensitized B cells. Online supplemental videos are available at http://www.jem.org/cgi/content/full/jem.20020201/DC1.

Results

CXCR4 Functions in Lymphocyte Homing to Lymph Nodes and Peyer's Patches. Although previous studies have not identified a role for CXCR4/CXCL12 in B cell homing, we considered the possibility that the function of this receptor–ligand pair in HEV attachment may have been masked by partial redundancy with CCR7 and its ligands, CCL19/CCL21. To test this possibility, we transferred splenocytes from mice reconstituted with $CXCR4^{+/+}$ or $CXCR4^{-/-}$ fetal liver cells to wild-type or CCL19- and CCL21-deficient B6-*plt/plt* mice. As shown in Fig. 1, the accumulation of $CFSE^+$ CXCR4–deficient B cells in the lymph nodes was dramatically suppressed in B6-*plt/plt* mice but not in wild-type mice, whereas $CFSE^+$ $CXCR4^{+/+}$ as well as $Ly5^{a+}$ internal control B cells accumulated in the lymph nodes of B6-*plt/plt* mice as efficiently as in wild-type mice. In Peyer's patches, similar ob-

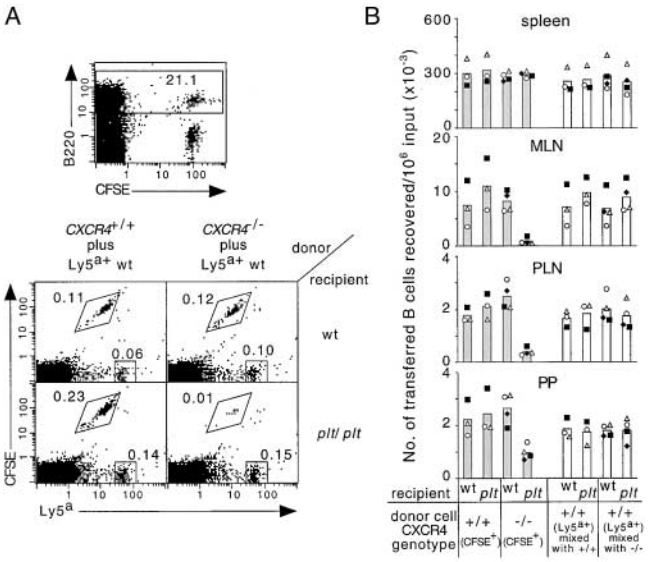

Figure 1. Defective homing of CXCR4-deficient B cells to lymph nodes and Peyer's patches of B6-*plt/plt* mice. (A) Representative flow cytometric analysis of transferred B cell accumulation in mesenteric lymph nodes of wild-type (wt) and B6-*plt/plt* recipients. $CXCR4^{+/+}$ or $CXCR4^{-/-}$ splenocytes were CFSE labeled, mixed with wild-type control $Ly5^{a+}$ splenocytes, and transferred into recipients for 90 min. Flow cytometric analysis of cells from a wild-type recipient of $CXCR4^{+/+}$ plus $Ly5^{a+}$ cells to show the separation of CFSE-labeled B and T cells, and the B220-gate (top). B220-gated cells plotted against CFSE fluorescence and $Ly5^a$ expression (bottom). Genotype of donor cell mixtures are indicated above the plots and recipient genotypes are indicated on the right of the plots. Gates demarcate the positions of $CFSE^+Ly5^{a-}$ and $CFSE^-Ly5^{a+}$ cells, and the numbers next to boxes indicate the percentage of total cells. (B) Enumeration of donor $CXCR4^{+/+}CFSE^+Ly5^{a-}$ B cells, $CXCR4^{-/-}CFSE^+Ly5^{a-}$ B cells (shaded columns) and $CFSE^-Ly5^{a+}$ internal control B cells (open columns) recovered from spleen, mesenteric lymph nodes, inguinal and axillary lymph nodes, or four Peyer's patches of wild-type and B6-*plt/plt* recipients 90 min after transfer. Data are expressed as the number of $CXCR4^{+/+}$, $CXCR4^{-/-}$, or internal control B cells recovered in each recipient per 10^6 respective B cells transferred. Each symbol type represents an individual experiment. Columns show means of these individual data points. The number of transferred $CXCR4^{-/-}$ cells in B6-*plt/plt* recipient mesenteric lymph nodes, inguinal and axillary lymph nodes, and Peyer's patches was significantly lower than the number of $CXCR4^{-/-}$ cells in wt recipients ($P < 0.01$ in each case, paired *t* test), and significantly lower than the number of $CXCR4^{+/+}$ and $Ly5^{a+}$ wild-type cells in B6-*plt/plt* recipients ($P < 0.005$ in each case, Student's *t* test). wt, wild type; MLN, mesenteric lymph nodes; PLN, inguinal and axillary lymph nodes; PP, Peyer's patches.

Published June 24, 2002

servations were obtained, although the suppression of B cell homing by the blockade of these chemokine signals was less pronounced than in lymph nodes (Fig. 1 B). The effect of CXCR4 deficiency was selective to lymph nodes and Peyer's patches, as similar numbers of mutant and wild-type cells were found in the spleen (Fig. 1 B) and blood (unpublished data).

Consistent with earlier reports (15, 16, 18, 27), the homing of wild-type T cells to lymph nodes and Peyer's patches was suppressed in B6-*plt/plt* mice (Fig. 2 A). Significantly, the remaining accumulation of T cells that occurred in the lymphoid organs of B6-*plt/plt* mice was almost completely abolished when the donor cells were CXCR4 deficient (Fig. 2 A). In contrast, CXCR4-deficient T cells accumulated normally in the lymphoid organs of wild-type mice (Fig. 2 A). In the course of these studies, it became evident that the suppression of T cell homing in B6-*plt/plt* mice was less severe than in the prior studies that had been performed in BALB/c- and DDD/1-*plt/plt* mice (15, 16, 18), and a direct comparison of T cell homing in B6- and BALB/c-*plt/plt* mice confirmed that T cell homing was more severely compromised in BALB/c-*plt/plt* mice (Fig. 2, A and B). The basis for this difference is unclear but may reflect a higher expression of the CCL21-leu gene in B6-*plt/plt* mice, or a greater transport of CCL21-leu produced in lymphatic vessels to lymph nodes. Consistent with the latter possibility, T cell homing to Peyer's patches, a tissue that does not receive afferent lymph, was similarly affected in B6- and BALB/c-*plt/plt* recipients (Fig. 2). Therefore, our observations establish that CXCR4 and CXCL12 can contribute to in vivo T cell homing, but at the same time they indicate that this pathway can, at most, support only a small amount of the normal homing mediated by CCR7–CCL19/CCL21.

Analysis of B cell homing in BALB/c-*plt/plt* mice revealed a twofold suppression in homing to lymph nodes and little suppression in homing to Peyer's patches in 90-min transfer experiments (unpublished data). In experiments in which we transferred CCR7-deficient B cells to B6 recipients, we observed a similar twofold inhibition in B cell homing to lymph nodes (Fig. 3 A) consistent with previous findings (17), and a lack of significant inhibition in homing to Peyer's patches (Fig. 3 A). The greater inhibition in lymph node homing in these experiments compared with the observations in B6-*plt/plt* mice (Fig. 1) is consistent with the interpretation that low amounts of CCL21 are present in B6-*plt/plt* lymph nodes. Importantly, however, the defect in CXCR4-deficient B cell homing in B6-*plt/plt* mice (Fig. 1 B) was substantially greater then the defect in CCR7-deficient B cell homing (Fig. 3 A).

As a further approach to test whether there was a combined requirement for CXCR4 and CCR7 in B cell homing, and to exclude the possible effects caused by the altered development of cells or lymphoid tissues in gene-deficient animals, we tested the homing of chemokine-desensitized wild-type lymphocytes in wild-type B6 mice. In agreement with the transfer studies in B6-*plt/plt* mice, the pretreatment of splenocytes with CCL19 and CXCL12 markedly suppressed B cell homing to lymph nodes, whereas the pretreatment with either chemokine alone caused only a small or no reduction of B cell homing ability (Fig. 3 B). Chemokine pretreatment did not have significant effects on cell accumulation in the spleen (Fig. 3, B and C), and treated and untreated cells were found in similar frequencies in the blood (unpublished data). Typi-

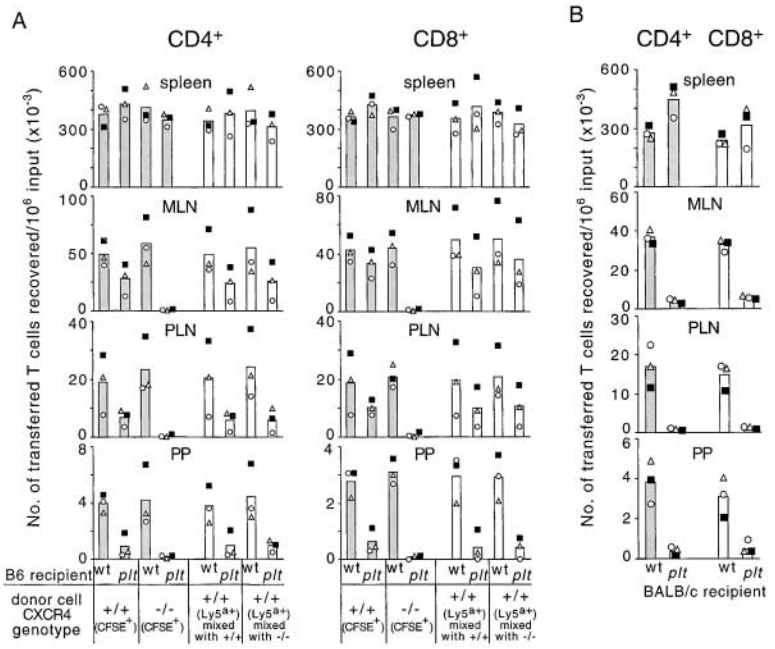

Figure 2. CXCR4-dependent accumulation of T cells in lymph nodes and Peyer's patches of B6-*plt/plt* mice and T cell homing in BALB/c-*plt/plt* mice. (A) Enumeration of donor CXCR4$^{+/+}$ or CXCR4$^{-/-}$ CD4 and CD8 T cells (shaded columns) and internal control CD4 and CD8 T cells (open columns) recovered from spleen, mesenteric lymph nodes, inguinal and axillary lymph nodes, or four Peyer's patches of wild-type and B6-*plt/plt* recipients 90 min after transfer. CXCR4$^{+/+}$ or CXCR4$^{-/-}$ T cells were identified as CD3$^+$CFSE$^+$Ly5^{a-} and internal control T cells as CD3$^+$CFSE$^-$Ly5^{a+}. These data are from three of the animals shown in Fig. 1. (B) Enumeration of donor CFSE$^+$CD4$^+$ or CFSE$^+$CD8$^+$ BALB/c T cells in BALB/c-*plt/plt* recipient tissues 90 min after transfer. Each symbol type represents an individual experiment and columns show means of these individual data points. The number of transferred wild-type CD4 and CD8 T cells in B6-*plt/plt* recipient mesenteric lymph nodes, inguinal and axillary lymph nodes, and Peyer's patches was significantly lower than the number that reached these tissues in wild-type recipients ($P < 0.01$ in each case, paired *t* test). The number of transferred CXCR4$^{-/-}$ CD4 and CD8 cells in B6-*plt/plt* recipient mesenteric lymph nodes, inguinal and axillary lymph nodes, and Peyer's patches was significantly reduced compared with the number of CXCR4$^{+/+}$ and Ly5^{a+} wild-type cells reaching these organs in B6-*plt/plt* recipients ($P < 0.03$ in each case, Student's *t* test). MLN, mesenteric lymph nodes; PLN, inguinal and axillary lymph nodes; PP, Peyer's patches.

Published June 24, 2002

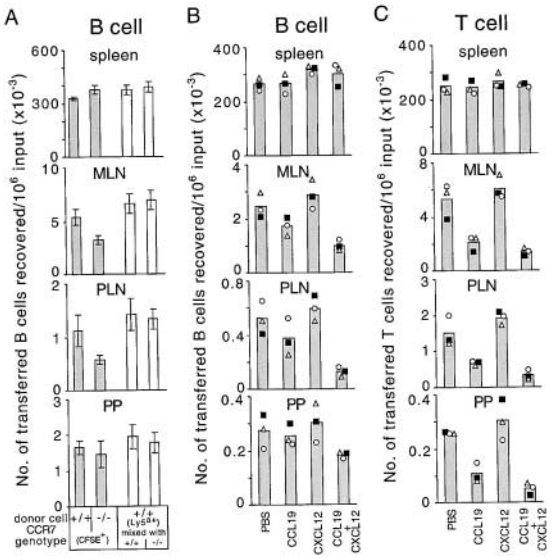

Figure 3. Suppression of B and T cell homing by desensitization of CCR7 and CXCR4. (A) Enumeration of donor $CCR7^{+/+}CFSE^{+}Ly5^{a-}$ B cells, $CCR7^{-/-}CFSE^{+}Ly5^{a-}$ B cells (shaded columns), and $CFSE^{-}Ly5^{a+}$ internal control B cells (open columns) recovered from spleen, mesenteric lymph nodes, inguinal and axillary lymph nodes, or four Peyer's patches of wild-type recipients 90 min after transfer (mean ± SD; $n = 7$). The number of $CCR7^{-/-}$ B cells reaching mesenteric lymph nodes and inguinal and axillary lymph nodes was significantly reduced compared with $CCR7^{+/+}$ cells ($P < 0.05$, paired t test). (B) Enumeration of donor $CFSE^{+}$ B cells and (C) donor $CFSE^{+}$ T cells, which had been incubated with PBS, 10 μg/ml CCL19 (ELC), 10 μg/ml CXCL12 (SDF1), or a combination of CCL19 and CXCL12 (10 μg/ml each) at 37°C for 45 min before transfer, recovered from spleen, mesenteric lymph nodes, inguinal lymph nodes, or three Peyer's patches (PP) of wild-type recipients 20 min after transfer. Each symbol type represents an individual experiment and columns show means of these individual data points. The number of CCL19 + CXCL12 pretreated B cells reaching mesenteric lymph nodes and inguinal lymph nodes was significantly reduced compared with PBS treated cells ($P < 0.05$, paired t test), whereas the effect in Peyer's patches did not reach statistical significance ($P = 0.09$). The number of CCL19 + CXCL12 pretreated T cells reaching inguinal and axillary lymph nodes was significantly reduced compared with CCL19 pretreated T cells ($P < 0.05$), whereas the effect in mesenteric lymph nodes and Peyer's patches was not statistically significant ($P = 0.07$ and 0.15, respectively). MLN, mesenteric lymph nodes; PLN, inguinal and axillary lymph nodes; PP, Peyer's patches.

cally, the desensitization method did not cause the same extent of inhibition in lymph node and Peyer's patch homing as the genetic deficiencies, which most likely reflects the incomplete desensitization or resensitization of some of the cells toward the end of the 20-min transfer time. Also, in agreement with the genetic studies, the suppression of B cell homing to Peyer's patches by desensitization of CCR7 and CXCR4 was not as prominent as the effect on B cell homing to lymph nodes (Fig. 3 B). As expected, T cell homing to lymph nodes and Peyer's patches was strongly diminished by pretreatment with CCL19 alone but not CXCL12 alone. Importantly, combined CXCL12 and CCL19 treatment led to a significantly greater inhibition in homing to peripheral lymph nodes than CCL19 treatment alone (Fig. 3 C). A similar trend was also observed for mesenteric lymph nodes and Peyer's patches, although in these cases the effect did not reach statistical significance.

HEV-associated Localization of CXCL12 in Lymph Nodes and Peyer's Patches. The above results suggested that CXCL12, as well as CCR7 ligands, was localized on HEVs. To test this possibility, we performed in situ hybridization and immunohistochemical analyses of CXCL12 expression. Strong CXCL12 mRNA expression was detected in medullary cords as previously reported (22). In addition, we observed CXCL12-expressing cells tightly associated with $PNAd^{+}$ HEVs in both lymph nodes (Fig. 4, A and B) and Peyer's patches (Fig. 4, D and E). CXCL12-expressing cells were sparse in other areas of the T zone (Fig. 4, A–E) in contrast to the numerous CCL21-expressing T zone stromal cells (Fig. 4, C and F). We did not detect CXCL12 expression by HEV cells (Fig. 4, B and E), whereas CCL21 was expressed by these cells (Fig. 4, C and F) as previously reported (7). Immunohistochemical staining of adjacent sections for CXCL12 and PNAd revealed that CXCL12 protein is present on lymph node HEVs, including the lumenal side of these vessels (Fig. 4, G and J). The specificity of this staining was confirmed by the markedly diminished staining intensity when the antiserum was neutralized by preincubation with CXCL12 peptide (Fig. 4, I and L). A comparison of the pattern of staining by PNAd and CXCL12 indicated that most $PNAd^{+}$ vessels were also positive for CXCL12 (Fig. 4, G–I and unpublished data). Similar signals for CXCL12 were observed on Peyer's patch HEVs (unpublished data). B220 staining showed the presence of B cells around $CXCL12^{+}$ HEVs (Fig. 4, A, H, and K).

CXCR4 and CCR7 Are Involved in B Cell Attachment to HEVs. To assess directly whether CXCL12 and CCL19/CCL21 localized at HEVs triggers the arrest and firm adhesion of B cells undergoing selectin-mediated rolling interactions with the endothelium, we observed B cell behavior in superficial inguinal lymph nodes by intravital microscopy. The low number of B cells generated in CXCR4-deficient fetal liver chimeras precluded us from using this genetic system for intravital studies. Instead, we used chemokine-desensitized cells, an approach previously used successfully to study chemokine requirements for T lymphocyte attachment to HEVs (15, 16). Because the ability of HEVs to support lymphocyte rolling and firm adhesion varies with the size of the vessel and possibly other parameters, we injected chemokine-treated and PBS-treated B cells, which had been loaded with 10-fold different concentrations of CFSE, one after the other into the same mice and observed their behavior in the identical vessel branches. As shown in Fig. 5, A–C, rolling fractions of PBS-treated B cells and B cells treated with a combination of CCL19 and CXCL12 were similar. Strikingly, the fraction of chemokine-desensitized B cells that arrested and became firmly adherent was 3.4-fold lower than that of control B cells (Fig. 5, A, B, and D). These observations establish that the chemokine signals through CCR7 and CXCR4 are involved in the mechanism that triggers B cell arrest and firm adhesion to HEVs.

Published June 24, 2002

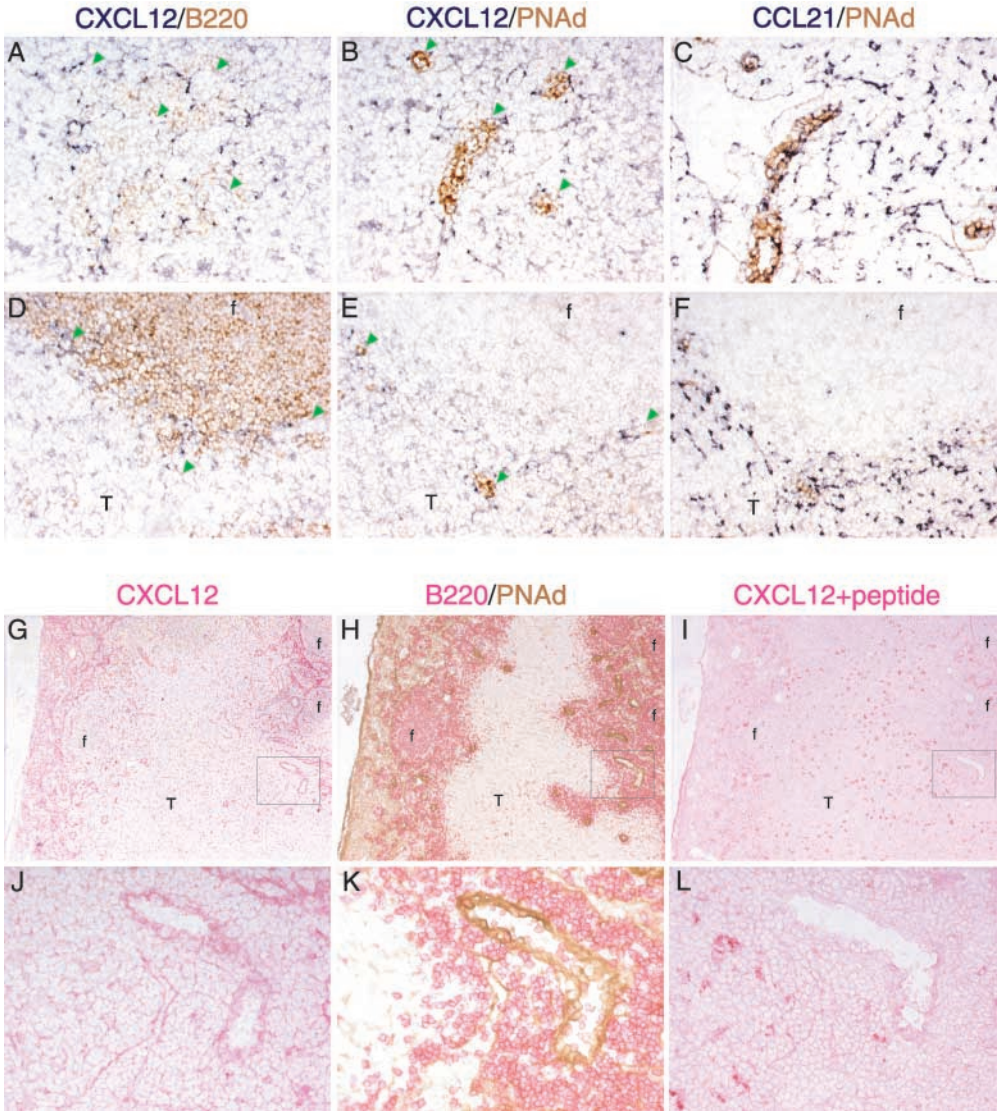

Figure 4. Detection of CXCL12 (SDF1) on HEVs in lymphoid organs. (A–F) In situ hybridization analysis of CXCL12 and (C and F) CCL21 (SLC) mRNA expression (dark blue) in adjacent sections (A–C) of a mesenteric lymph node and (D–F) a Peyer's patch in combination with immunohistochemical staining (brown) for (A and D) B220 and (B, C, E, and F) PNAd to detect B cells and HEVs, respectively. Green arrowheads in A, B, D, and E indicate the positions of HEVs. Objective magnification, ×20. (G–L) Immunohistochemical analysis of CXCL12 protein distribution in lymph nodes. Adjacent sections of mesenteric lymph node were stained with anti-CXCL12 (G and J, red), anti-B220 (H and K, red), anti-PNAd (H and K, brown), and anti-CXCL12 antibody preincubated with CXCL12 blocking peptide (I and L, red). (J–L) High magnification images of the boxed areas in G–I. f, follicle; T, T zone. Objective magnification: G–I, ×5; J–L, ×20.

CXCR5 and CXCL13 Contribute to the B Cell Homing Mechanism in Peyer's Patches. In contrast to the findings in lymph nodes, transferred B cells accumulated in Peyer's patches to considerable numbers, even when both CCR7 and CXCR4 signaling was blocked (Figs. 1 and 3). These findings suggested that additional chemokine signals were involved in B cell entry to Peyer's patches. As CXCL13 is highly expressed in Peyer's patches, and CXCL13 and CXCR5 are important for normal development of Peyer's patches, it seemed possible that this chemokine–receptor pair might be involved in B cell entry to this organ. By immunohistochemical analyses, CXCL13 was not detected at HEVs near the edges or outside of follicles. However, we found $CXCL13^+$ HEVs located inside follicles where CXCL13 is abundantly expressed (Fig. 6 A). These $CXCL13^+$ HEVs were $MAdCAM^+$ and were typically smaller than those in the T zones (Fig. 6 B). Previous studies have shown that a fraction of the B cells entering Peyer's patches migrate through small vessels located within follicles (16, 28). Equivalently CXCL13-stained vessels were not observed in lymph nodes (unpublished data).

To test whether CXCR5 played a role in B cell homing to Peyer's patches, we transferred splenocytes from $CXCR5^{-/-}$ or wild-type mice with splenocytes from $Ly5^{a+}$ mice to wild-type recipients. As shown in Fig. 6 C, the accumulation of CXCR5-deficient B cells in Peyer's patches in 90 min was significantly diminished, whereas the homing to lymph nodes and spleen was hardly affected by the CXCR5 deficiency of B cells. In control experiments, the accumulation of B cells from $CXCL13^{-/-}$ mice in wild-type Peyer's patches was similar to that of wild-type B cells, establishing that the lack of Peyer's patches in donor mice was not the cause of the suppressed homing of CXCR5-deficient B cells (Fig. 6 C, ■). As expected, the homing of $CXCR5^{-/-}$ T cells to Peyer's patches was indistinguishable from wild-type controls (unpublished data). To further test whether CXCR4, CXCR5, and CCR7 were the principal chemokine receptors involved in the B

Published June 24, 2002

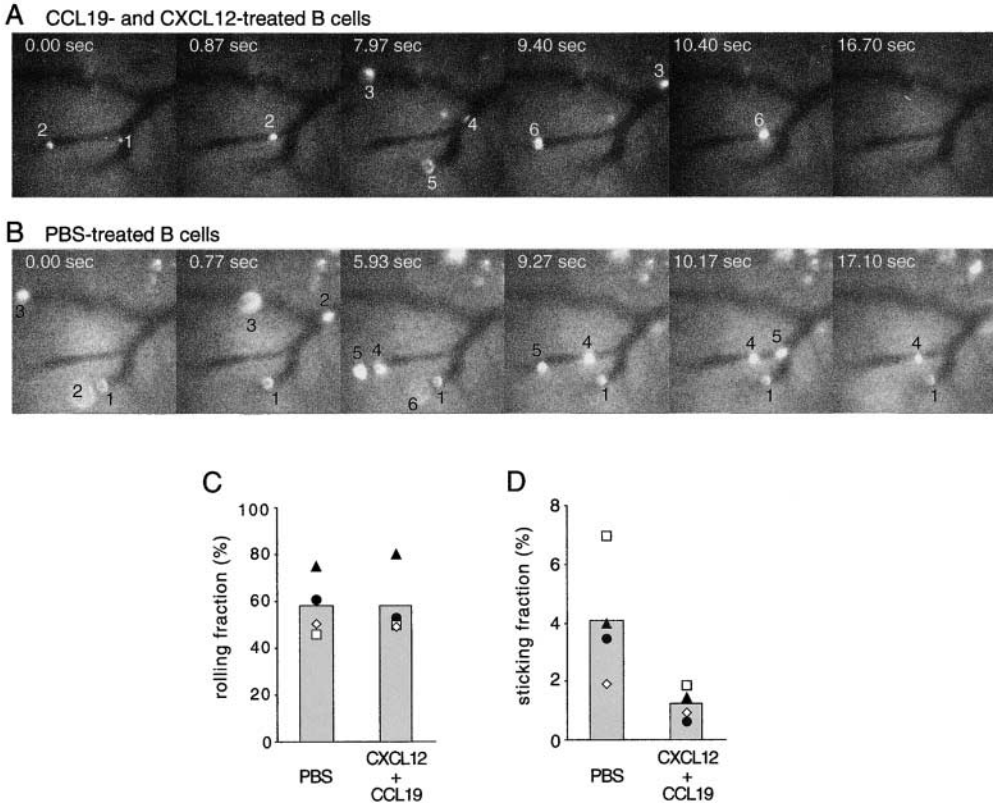

Figure 5. Combined desensitization of CXCR4 and CCR7 prevents B cell arrest on lymph node HEVs. (A) Representative time-lapse intravital micrographs of superficial inguinal lymph node HEVs, in which transferred 2-μM CFSE-labeled, chemokine-desensitized B cells flowed and rolled. Donor B cells had been incubated with a combination of CCL19 and CXCL12 (10 μg/ml each) before transfer. Transferred cells appearing in the vessel branches are numbered in their order of appearance. The time elapsed, starting from the first frame shown, is indicated in each image. B cells numbered 1–3 and 6 rolled on HEVs, but none of the cells became arrested. (B) Representative time-lapse intravital micrographs of the same superficial inguinal lymph node HEVs as in A, after secondary injection of 20-μM CFSE-labeled B cells, which had been incubated with PBS. B cells numbered 1 and 3–5 rolled on HEVs, and 1 and 4 were arrested on HEVs until the end of recording (~5 min; see Videos 1 and 2 available at http://www.jem.org/cgi/content/full/jem.20020201/DC1). (C and D) Fractions of B cells passing through HEVs that were recorded as (C) rolling or (D) arrested. B cells had been pretreated with PBS or with combined CCL19 and CXCL12 as in A and B. Arrested B cells were defined as cells that were adherent for greater than 1 min. Open symbols represent data from experiments in which chemokine-desensitized cells were injected first, and filled symbols represent data from experiments in which PBS-treated cells were injected first. Columns show means of the individual datasets. The number of CXCL12 + CCL19 pretreated cells that stuck was significantly reduced ($P = 0.04$, paired t test).

cell homing to Peyer's patches, CXCR5-deficient cells were pretreated with CCL19 and CXCL12, and transferred to wild-type recipients for 20 min. Compared with wild-type cells, in which 270 ± 36 cells per 10^6 transferred cells homed to Peyer's patches in these very short-term experiments, 44% fewer (150 ± 4; $n = 3$) CXCR5-deficient cells and 63% fewer (100 ± 7; $n = 3$) CCL19 + CXCL12 pretreated CXCR5–deficient cells accumulated in Peyer's patches during this time. The studies above (Figs. 1 and 3), comparing the homing of CXCR4-deficient cells in B6-*plt/plt* mice and of CCL19 + CXCL12 pretreated wild-type cells in wild-type mice, showed that the chemokine pretreatment approach only caused a partial inhibition of CCR7- and CXCR4-mediated homing. Taken together, these findings favor the conclusion that CXCR5, CXCR4, and CCR7 account for the majority of the chemokine receptor requirements for B cell homing to Peyer's patches, with CXCR5 playing a limited role, and CCR7 and CXCR4 making redundant contributions.

The CXCL13-staining pattern (Fig. 6 A) suggested that the CXCL13–CXCR5 ligand–receptor pair may be selectively required for B cells to attach to HEVs within Peyer's patch follicles. To test this possibility, we cotransferred TRITC-labeled wild-type and CFSE-labeled CXCR5-deficient B cells into wild-type mice and examined their distribution within Peyer's patches 20 min later by whole mount microscopy (Fig. 6, D–F). Consistent with previous findings (16, 28), wild-type B cells were found to attach to vessels within follicles in addition to the larger vessels in T cell areas (Fig. 6, D–F, red cells). In contrast, CXCR5-deficient B cells failed to accumulate in vessels within B cell follicles, although they could be observed associated with vessels in T cell areas (Fig. 6, D–F, green cells). These results reveal a selective role for CXCL13 and CXCR5 in B cell homing via follicle-associated HEVs into Peyer's patches.

Discussion

The above results establish that CCR7 and CXCR4 are the major chemokine receptors involved in B cell entry into lymph nodes. In Peyer's patches, an additional chemokine receptor, CXCR5, contributes nonredundantly to B cell homing. CXCR4 is also able to support a low level of T cell homing to lymph nodes and Peyer's patches when CCR7 ligands are deficient. Messenger RNA for the CXCR4 ligand, CXCL12, was identified in cells adjacent to HEVs, and CXCL12 protein was detectable on the lumenal surface of HEVs. CXCL13, the ligand for CXCR5, was detected on a subset of Peyer's patch but not lymph node HEVs. Taken together, these studies define the

Published June 24, 2002

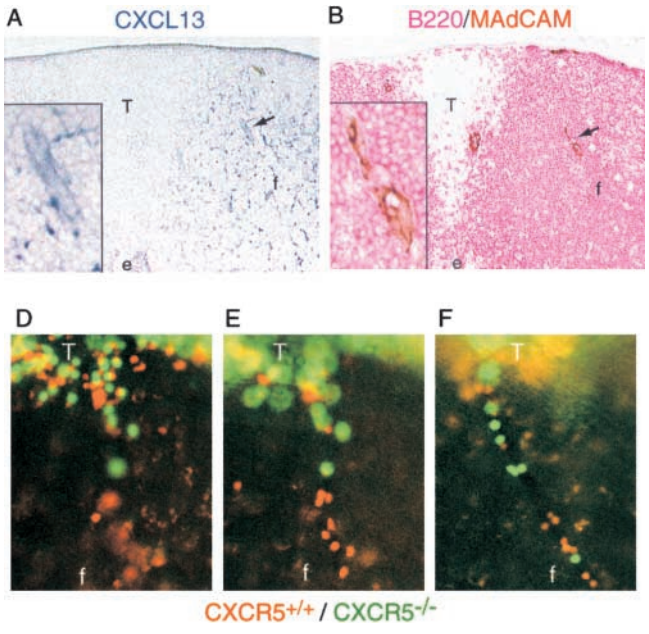

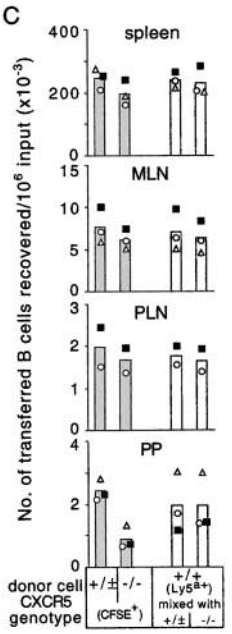

Figure 6. Involvement of CXCL13 (BLC) and CXCR5 in B cell homing to Peyer's patches. (A and B) Immunohistochemical analysis of CXCL13 distribution in Peyer's patches. Adjacent Peyer's patch sections were stained for (A) CXCL13 (blue), or B220 (red), and (B) MAdCAM (brown). A $CXCL13^+$ HEV is indicated by the arrow, and higher magnification images of this vessel are shown in the insets. e, epithelium; f, follicle; T, T zone. Objective magnification, ×10 (insets, ×40). (C) Enumeration of donor $CXCR5^{+/\pm}CFSE^+$ B cells, $CXCR5^{-/-}CFSE^+$ B cells (shaded columns) and $CFSE^-Ly5^{a+}$ internal control B cells (open columns) recovered from spleen, mesenteric lymph nodes, inguinal and axillary lymph nodes, or four Peyer's patches of wild-type recipients 90 min after transfer. In the transfer experiment shown by the filled squares, the $CXCR5^{+/+}$ donor was $CXCL13^{-/-}$. The number of transferred $CXCR5^{-/-}$ cells in Peyer's patches was significantly lower than the number of $CXCR5^{+/+}$ cells ($P < 0.001$, paired t test). Similar findings were obtained in a separate experiment using $CXCL13^{+/-}$ recipients. MLN, mesenteric lymph nodes; PLN, inguinal and axillary lymph nodes; PP, Peyer's patches. (D–F) Whole mount microscopy of Peyer's patches from mice that had received CFSE-labeled $CXCR5^{-/-}$ and TRITC-labeled wild-type B cells 20 min earlier. Images in D and E are of the same field at different focal planes to provide detail of cells in the (D) T zone versus the (E) follicle. F shows a view of a vessel within another Peyer's patch. Objective magnification, ×20. The location of follicles and T cell areas was determined by orientating the Peyer's patch under low magnification (×5) and comparing the image with images obtained from similarly orientated Peyer's patches from animals that had received fluorescently labeled T cells. The data in D–F are representative of vessels observed in more than 10 Peyer's patches in three experiments. f, follicle; T, T cell.

chemokine code required for B cell trafficking into peripheral lymphoid organs (Fig. 7).

CCL21 was the first chemokine shown to be made by HEVs, and it is present at high levels on the abluminal and lumenal surface of HEVs as well as within T cell areas (7, 15, 16). Expression of CCL19, by contrast, has not been detected in endothelial cells (25). However, CCL19 is expressed by T zone stromal cells surrounding HEVs (13, 25), and CCL19 protein has been reported to be transcytosed by endothelial cells and presented on the lumenal side of HEVs (8). Earlier studies established that CXCL8 (IL-8) was efficiently transcytosed and displayed by endothelial cells (29), and more recently CCL2 (MCP1) and CXCL9 (MIG) have been found to be transcytosed and displayed by HEVs (30, 31). In this study, we show that CXCL12, like CCL19, is not detectably expressed by HEVs, but is expressed by cells adjacent to HEVs and is displayed on the HEV lumen. The nature of the CXCL12-expressing cell type is presently unclear, although it is interesting that in human skin CXCL12 has been identified in the pericytes that surround endothelial cells (32). Although not previously reported on HEVs, CXCL12 has been observed on skin endothelial cells (32), bone marrow endothelial cells (33), and endothelium within the rheumatoid synovium (34). Additional studies are needed to determine the mechanism by which CXCL12 is transcytosed and displayed by endothelial cells. In the case of $CXCL13^+$ HEVs in Peyer's patches, it is currently unclear whether the follicular HEVs express CXCL13 mRNA. However, large amounts of CXCL13 are made by stromal cells throughout the follicle and it seems likely that at least a fraction of the chemokine displayed by the follicular HEVs is derived from the surrounding stromal cells. Recently, $CXCL13^+$ HEVs were identified in human tonsil (35), a B cell–rich mucosal lymphoid tissue that has similar features to Peyer's patches, which indicates that the display of CXCL13 by follicular HEVs in such tissues is a conserved property between mice and humans. Peyer's patches and tonsils are chronically activated and usually contain many germinal centers. It will be interesting to determine whether antigen-induced responses promote transcytosis and display of CXCL13 on follicle-associated HEVs.

Our experiments show that when the chemokine signals through both CCR7 and CXCR4 are reduced or blocked, B cell accumulation in the lymph nodes is decreased ~90% compared with wild-type levels (Fig. 1). This extent of inhibition approached that observed for B cells treated with pertussis toxin, in which the number of treated cells recovered from lymph nodes was reduced by ~95% in short-term transfer experiments (unpublished data). Therefore, CCR7 and CXCR4 are responsible for the majority of Gi-coupled signaling required for B cell homing to lymph nodes during homeostasis. Our findings and previous studies (17) indicate that when B cells are deficient only in CCR7 they have a partial reduction in lymph node homing, whereas CXCR4 deficiency alone did not cause a measurable loss of homing ability. Similar conclusions were suggested by our findings with chemokine-desensitized wild-type cells, in which CCL19 desensitization caused a small decrease in homing to wild-type lymph nodes, whereas CXCL12 desensitization alone did not affect hom-

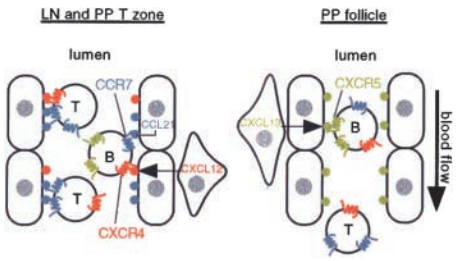

Figure 7. Principal chemokine requirements for B and T cell entry into lymph nodes and Peyer's patches. The diagram represents a lymph node or Peyer's patch T zone HEV on the left and a Peyer's patch follicular HEV on the right. CCL21 (SLC) is expressed by endothelial cells (oval shaped), whereas CXCL12 (SDF1) is expressed by stromal cells (triangular shaped) juxtaposed to HEVs. Both chemokines are presented on the lumenal side of HEVs. CCL19 (ELC) expressed by T zone stromal cells may also be presented on these HEVs (not shown). Large amounts of chemokine are also present in an abluminal location (not shown). CCR7 plays an indispensable role in triggering T cell adhesion, and CXCR4 can contribute partially to this process. B cells are triggered to adhere by either CCR7 or CXCR4, with CCR7 supporting approximately twofold more adhesion triggering events than CXCR4. Follicular areas of Peyer's patches contain HEVs of a smaller diameter than the T zone HEVs, and these vessels display CXCL13 (BLC), most likely derived from follicular stromal cells, although CXCL13 may also be expressed by the endothelial cells. B cells are triggered to adhere to these vessels by CXCL13/CXCR5. CXCR5 supports ~50% of the chemokine triggering requirement for B cell homing to Peyer's patches. Most T cells do not express CXCR5 and are not triggered to adhere to HEVs in follicles, passing through to T zone HEVs where they may be arrested. T, T cells; B, B cells.

ing. Therefore, the role of CCR7 in B cell entry to lymph nodes and Peyer's patches appears to be partially redundant with CXCR4, whereas the contribution of CXCR4 appears to be fully redundant with CCR7.

In contrast to lymph nodes, Peyer's patch homing was only ~50% affected by the combined blockade of CCR7 and CXCR4. However, when B cells were selectively deficient in CXCR5, there was also about a twofold decrease in Peyer's patch homing (Fig. 6). CXCR5-deficient cells that had been pretreated with CCL19 and CXCL12 showed a more complete (~63%) block in homing. We consider that our inability to fully block Peyer's patch homing by this approach was due to the incomplete inhibition achieved by chemokine pretreatment, but at the present time we cannot exclude a small contribution to Peyer's patch homing by an additional chemokine. Decreased Peyer's patch homing was not reported in earlier studies of CXCR5 and CXCL13 deficient mice, most likely because animals with endogenous deficiencies in these genes have severe defects in early steps of Peyer's patch development and have few, if any, Peyer's patches (20, 21). In other studies, it was observed that B cells preferentially attach to HEVs within Peyer's patch follicles, at the borders of follicles, and at T cell areas, whereas T cells enter preferentially via HEVs in T cell areas (16, 28). CCL21 was found to be selectively expressed by HEVs in T cell areas and follicle-associated HEVs showed minimal CCL21 expression (16). Taking these observations together with our finding that $CXCL13^+$ HEVs are limited to follicles, and that the CXCR5 contribution to B cell Peyer's patch homing was nonredundant, it appeared likely that CXCR5 and CXCL13 would play a limiting role in B cell attachment to follicle-associated HEVs. This was confirmed by whole mount microscopy analysis, in which CXCR5-deficient B cells were found to be inefficient in attachment to follicle-associated HEVs. Therefore, we propose that the CXCR5–CXCL13 receptor–ligand pair plays a selective role in B cell trafficking across HEVs within Peyer's patch follicles (Fig. 7).

In agreement with other studies (36, 37), we observed differences in the relative efficiency of B and T cell entry to Peyer's patches compared with lymph nodes. Although T cells home to lymph nodes and Peyer's patches more efficiently than B cells, the difference in efficiency was 5–10-fold for lymph nodes but less than twofold for Peyer's patches (compare Figs. 1 and 2). The greater relative efficiency of B cell homing to Peyer's patches compared with lymph nodes was mostly lost when the cells lacked CXCR5 (Fig. 6). Therefore, we conclude that differences in the HEV chemokine code contribute to differences in the efficiency of B and T lymphocyte homing to different lymphoid organs. These differences, along with differences in B and T cell retention time within the tissue (37), may contribute to the greater predominance of B than T cells in Peyer's patches.

Our results show that CXCR4 is able to function in T cell homing to lymph nodes and Peyer's patches. However, as established in past studies (17, 18), CCR7 and its ligands play a dominant role in T cell homing (Fig. 7), and the contribution of CXCR4 appears to be fully redundant with CCR7. The difference in the chemokine dependence of T and B cells for homing may reflect the differential responsiveness to CCL19/CCL21 with relatively similar responsiveness to CXCL12. T cells express ~10-fold higher surface levels of CCR7 than B cells (unpublished data) and they are substantially more responsive to the respective ligands in in vitro chemotaxis assays (7, 25). Both CCL19 and CCL21 have been shown to promote T and B lymphocyte adhesion to intercellular adhesion molecule 1 (ICAM1; references 9 and 10) and MAdCAM1 (38). CXCL12 has been shown to promote adhesion of peripheral blood lymphocytes to ICAM1 (9, 10), although direct tests of purified B cells have not been reported. It will be interesting to determine whether T cells are more sensitive than B cells in their CCL19 and CCL21 concentration requirements for triggering integrin-mediated adhesion to ICAM1 and MAdCAM1.

As already noted, a well-established feature of lymphocyte homing is that T cells enter lymph nodes with considerably greater efficiency than B cells (compare Figs. 1 and 2; references 36 and 37). One mechanism contributing to this difference appears to be the higher expression of L-selectin on T cells compared with B cells (37). We propose that another mechanism is the greater responsiveness of T cells to CCL19/CCL21 than B cells coupled with the high concentration of CCL21 on lymph node HEVs. Consistent with the chemokine triggering step contributing to the differing efficiency of T and B cell homing, the fraction of rolling B cells that underwent arrest in lymph node HEVs

(Fig. 5 and supplemental Quicktime videos available at http://www.jem.org/cgi/content/full/jem.20020201/DC1) was lower than that observed for T cells (6, 15).

An additional implication of our findings is that T cells that have modulated CCR7 expression may be able to continue entering lymph nodes and Peyer's patches via the CXCR4 pathway. Although memory T cells often modulate CXCR4 (39, 40), some memory cells maintain expression (41). A fraction of circulating memory T cells also express CXCR5 (42, 43). Other circulating cell types that are CCR7-low or -negative and that express CXCR4 or CXCR5, such as monocytes and immature dendritic cells (40, 44), may also be able to use these receptors for triggering adhesion to endothelium.

In summary, CCR7 and CXCR4 are the major receptors providing the triggering signals for B cell entry into lymph nodes, and CXCR5 as well as CXCR4 and CCR7 provide the triggering signals for B cell entry into Peyer's patches (Fig. 7). The presence of large amounts of the ligands for each of these receptors on the abluminal side of HEVs, in addition to the lumenal side, suggests that they may function both in triggering firm adhesion of rolling cells and in the subsequent diapedesis step. Although a chemokine gradient may not be critical for diapedesis, a Gi-coupled receptor signal is needed (45). In addition to their expression in secondary lymphoid tissues, CXCL12 is expressed in bone marrow and in epithelial tissues, and both CXCL12 and CXCL13 have been identified at sites of chronic inflammation (33, 46). Our findings support a role for CXCL12 in promoting adhesion and transmigration of circulating stem and plasma cells across bone marrow endothelium, and in the entry of B cells and $CXCR4^+$ memory T cells to sites of inflammation (34, 41).

We thank Shaun Coughlin for use of the video microscope, Justin Hamilton, Ethan Weiss, and Mark Ansel for help with microscopy, Lars Ohl for bone marrow, and Sanjiv Luther and Steve Rosen for advice and critical review of the manuscript.

T. Okada is supported by the Japan Society for the Promotion of Science, J.G. Cyster is a Packard Fellow and a Howard Hughes Medical Institute Assistant Investigator. This work was supported in part by National Institutes of Health grant AI45073.

Submitted: 6 February 2002
Revised: 9 April 2002
Accepted: 14 May 2002

References

1. Springer, T.A. 1994. Traffic signals for lymphocyte recirculation and leukocyte emigration: the multistep paradigm. *Cell.* 76:301–314.
2. Butcher, E.C., and L.J. Picker. 1996. Lymphocyte homing and homeostasis. *Science.* 272:60–66.
3. Spangrude, G.J., B.A. Braaten, and R.A. Daynes. 1984. Molecular mechanisms of lymphocyte extravasation I. Studies of two selective inhibitors of lymphocyte recirculation. *J. Immunol.* 132:354–362.
4. Bargatze, R.F., and E.C. Butcher. 1993. Rapid G protein regulated activation event involved in lymphocyte binding to high endothelial venules. *J. Exp. Med.* 178:367–372.
5. Cyster, J.G., and C.C. Goodnow. 1995. Pertussis toxin inhibits migration of B and T lymphocytes into splenic white pulp cords. *J. Exp. Med.* 182:581–586.
6. Warnock, R.A., S. Askari, E.C. Butcher, and U.H. von Andrian. 1998. Molecular mechanisms of lymphocyte homing to peripheral lymph nodes. *J. Exp. Med.* 187:205–216.
7. Gunn, M.D., K. Tangemann, C. Tam, J.G. Cyster, S.D. Rosen, and L.T. Williams. 1998. A chemokine expressed in lymphoid high endothelial venules promotes the adhesion and chemotaxis of naive T lymphocytes. *Proc. Natl. Acad. Sci. USA.* 95:258–263.
8. Baekkevold, E.S., T. Yamanaka, R.T. Palframan, H.S. Carlsen, F.P. Reinholt, U.H. von Andrian, P. Brandtzaeg, and G. Haraldsen. 2001. The CCR7 ligand ELC (CCL19) is transcytosed in high endothelial venules and mediates T cell recruitment. *J. Exp. Med.* 193:1105–1112.
9. Campbell, J.J., J. Hedrick, A. Zlotnik, M.A. Siani, D.A. Thompson, and E.C. Butcher. 1998. Chemokines and the arrest of lymphocytes rolling under flow conditions. *Science.* 279:381–384.
10. Tangemann, K., M.D. Gunn, P. Giblin, and S.D. Rosen. 1998. A high endothelial cell-derived chemokine induces rapid, efficient, and subset-selective arrest of rolling T lymphocytes on a reconstituted endothelial substrate. *J. Immunol.* 161:6330–6337.
11. Gunn, M.D., S. Kyuwa, C. Tam, T. Kakiuchi, A. Matsuzawa, L.T. Williams, and H. Nakano. 1999. Mice lacking expression of secondary lymphoid organ chemokine have defects in lymphocyte homing and dendritic cell localization. *J. Exp. Med.* 189:451–460.
12. Vassileva, G., H. Soto, A. Zlotnik, H. Nakano, T. Kakiuchi, J.A. Hedrick, and S.A. Lira. 1999. The reduced expression of 6Ckine in the *plt* mouse results from the deletion of one of two 6Ckine genes. *J. Exp. Med.* 190:1183–1188.
13. Luther, S.A., H.L. Tang, P.L. Hyman, A.G. Farr, and J.G. Cyster. 2000. Coexpression of the chemokines ELC and SLC by T zone stromal cells and deletion of the ELC gene in the plt/plt mouse. *Proc. Natl. Acad. Sci. USA.* 97:12694–12699.
14. Nakano, H., and M.D. Gunn. 2001. Gene duplications at the chemokine locus on mouse chromosome 4: multiple strain-specific haplotypes and the deletion of secondary lymphoid-organ chemokine and EBI-1 ligand chemokine genes in the plt mutation. *J. Immunol.* 166:361–369.
15. Stein, J.V., A. Rot, Y. Luo, M. Narasimhaswamy, H. Nakano, M.D. Gunn, A. Matsuzawa, E.J. Quackenbush, M.E. Dorf, and U.H. von Andrian. 2000. The CC chemokine thymus-derived chemotactic agent 4 (TCA-4, secondary lymphoid tissue chemokine, 6Ckine, exodus-2) triggers lymphocyte function–associated antigen 1–mediated arrest of rolling T lymphocytes in peripheral lymph node high endothelial venules. *J. Exp. Med.* 191:61–76.
16. Warnock, R.A., J.J. Campbell, M.E. Dorf, A. Matsuzawa, L.M. McEvoy, and E.C. Butcher. 2000. The role of chemokines in the microenvironmental control of T versus B cell arrest in Peyer's patch high endothelial venules. *J. Exp. Med.* 191:77–88.
17. Förster, R., A. Schubel, D. Breitfeld, E. Kremmer, I. Renner-Muller, E. Wolf, and M. Lipp. 1999. CCR7 coordinates the primary immune response by establishing functional microenvironments in secondary lymphoid organs. *Cell.* 99:23–33.
18. Nakano, H., T. Tamura, T. Yoshimoto, H. Yagita, M. Mi-

yasaka, E.C. Butcher, H. Nariuchi, T. Kakiuchi, and A. Matsuzawa. 1997. Genetic defect in T lymphocyte-specific homing into peripheral lymph nodes. *Eur. J. Immunol.* 27:215–221.
19. Ma, Q., D. Jones, P.R. Borghesani, R.A. Segal, T. Nagasawa, T. Kishimoto, R.T. Bronson, and T.A. Springer. 1998. Impaired B-lymphopoiesis, myelopoiesis, and derailed cerebellar neuron migration in CXCR4- and SDF-1-deficient mice. *Proc. Natl. Acad. Sci. USA.* 95:9448–9453.
20. Förster, R., A.E. Mattis, E. Kremmer, E. Wolf, G. Brem, and M. Lipp. 1996. A putative chemokine receptor, BLR1, directs B cell migration to defined lymphoid organs and specific anatomic compartments of the spleen. *Cell.* 87:1037–1047.
21. Ansel, K.M., V.N. Ngo, P.L. Hyman, S.A. Luther, R. Förster, J.D. Sedgwick, J.L. Browning, M. Lipp, and J.G. Cyster. 2000. A chemokine driven positive feedback loop organizes lymphoid follicles. *Nature.* 406:309–314.
22. Hargreaves, D.C., P.L. Hyman, T.T. Lu, V.N. Ngo, A. Bidgol, G. Suzuki, Y.R. Zou, D.R. Littman, and J.G. Cyster. 2001. A coordinated change in chemokine responsiveness guides plasma cell movements. *J. Exp. Med.* 194:45–56.
23. Goodnow, C.C., J. Crosbie, S. Adelstein, T.B. Lavoie, S.J. Smith-Gill, R.A. Brink, H. Pritchard-Briscoe, J.S. Wotherspoon, R.H. Loblay, K. Raphael, et al. 1988. Altered immunoglobulin expression and functional silencing of self-reactive B lymphocytes in transgenic mice. *Nature.* 334:676–682.
24. Cyster, J.G., and C.C. Goodnow. 1995. Antigen-induced exclusion from follicles and anergy are separate and complementary processes that influence peripheral B cell fate. *Immunity.* 3:691–701.
25. Ngo, V.N., H.L. Tang, and J.G. Cyster. 1998. Epstein-Barr virus–induced molecule 1 ligand chemokine is expressed by dendritic cells in lymphoid tissues and strongly attracts naive T cells and activated B cells. *J. Exp. Med.* 188:181–191.
26. von Andrian, U.H. 1996. Intravital microscopy of the peripheral lymph node microcirculation in mice. *Microcirculation.* 3:287–300.
27. Nakano, H., S. Mori, H. Yonekawa, H. Nariuchi, A. Matsuzawa, and T. Kakiuchi. 1998. A novel mutant gene involved in T-lymphocyte-specific homing into peripheral lymphoid organs on mouse chromosome 4. *Blood.* 91:2886–2895.
28. Miura, S., Y. Tsuzuki, D. Fukumura, H. Serizawa, M. Suematsu, I. Kurose, H. Imaeda, H. Kimura, H. Nagata, M. Tsuchiya, et al. 1995. Intravital demonstration of sequential migration process of lymphocyte subpopulations in rat Peyer's patches. *Gastroenterology.* 109:1113–1123.
29. Middleton, J., S. Neil, J. Wintle, I. Clark-Lewis, H. Moore, C. Lam, M. Auer, E. Hub, and A. Rot. 1997. Transcytosis and surface presentation of IL-8 by venular endothelial cells. *Cell.* 91:385–395.
30. Janatpour, M.J., S. Hudak, M. Sathe, J.D. Sedgwick, and L.M. McEvoy. 2001. Tumor necrosis factor–dependent segmental control of MIG expression by high endothelial venules in inflamed lymph nodes regulates monocyte recruitment. *J. Exp. Med.* 194:1375–1384.
31. Palframan, R.T., S. Jung, G. Cheng, W. Weninger, Y. Luo, M. Dorf, D.R. Littman, B.J. Rollins, H. Zweerink, A. Rot, and U.H. von Andrian. 2001. Inflammatory chemokine transport and presentation in HEV: a remote control mechanism for monocyte recruitment to lymph nodes in inflamed tissues. *J. Exp. Med.* 194:1361–1373.
32. Pablos, J.L., A. Amara, A. Bouloc, B. Santiago, A. Caruz, M. Galindo, T. Delaunay, J.L. Virelizier, and F. Arenzana-Seisdedos. 1999. Stromal-cell derived factor is expressed by dendritic cells and endothelium in human skin. *Am. J. Pathol.* 155:1577–1586.
33. Peled, A., V. Grabovsky, L. Habler, J. Sandbank, F. Arenzana-Seisdedos, I. Petit, H. Ben-Hur, T. Lapidot, and R. Alon. 1999. The chemokine SDF-1 stimulates integrin-mediated arrest of CD34(+) cells on vascular endothelium under shear flow. *J. Clin. Invest.* 104:1199–1211.
34. Buckley, C.D., N. Amft, P.F. Bradfield, D. Pilling, E. Ross, F. Arenzana-Seisdedos, A. Amara, S.J. Curnow, J.M. Lord, D. Scheel-Toellner, et al. 2000. Persistent induction of the chemokine receptor CXCR4 by TGF-beta 1 on synovial T cells contributes to their accumulation within the rheumatoid synovium. *J. Immunol.* 165:3423–3429.
35. Schaerli, P., K. Willimann, A.B. Lang, M. Lipp, P. Loetscher, and B. Moser. 2000. CXC chemokine receptor 5 expression defines follicular homing T cells with B cell helper function. *J. Exp. Med.* 192:1553–1562.
36. Stevens, S.K., I.L. Weissman, and E.C. Butcher. 1982. Differences in the migration of B and T lymphocytes: organ-selective localization in vivo and the role of lymphocyte-endothelial cell recognition. *J. Immunol.* 128:844–851.
37. Tang, M.L., D.A. Steeber, X.Q. Zhang, and T.F. Tedder. 1998. Intrinsic differences in L-selectin expression levels affect T and B lymphocyte subset-specific recirculation pathways. *J. Immunol.* 160:5113–5121.
38. Pachynski, R.K., S.W. Wu, M.D. Gunn, and D.J. Erle. 1998. Secondary lymphoid-tissue chemokine (SLC) stimulates integrin alpha 4 beta 7-mediated adhesion of lymphocytes to mucosal addressin cell adhesion molecule-1 (MAdCAM-1) under flow. *J. Immunol.* 161:952–956.
39. Bleul, C.C., L. Wu, J.A. Hoxie, T.A. Springer, and C.R. Mackay. 1997. The HIV coreceptors CXCR4 and CCR5 are differentially expressed and regulated on human T lymphocytes. *Proc. Natl. Acad. Sci. USA.* 94:1925–1930.
40. Lee, B., M. Sharron, L.J. Montaner, D. Weissman, and R.W. Doms. 1999. Quantification of CD4, CCR5, and CXCR4 levels on lymphocyte subsets, dendritic cells, and differentially conditioned monocyte-derived macrophages. *Proc. Natl. Acad. Sci. USA.* 96:5215–5220.
41. Nanki, T., K. Hayashida, H.S. El-Gabalawy, S. Suson, K. Shi, H.J. Girschick, S. Yavuz, and P.E. Lipsky. 2000. Stromal cell-derived factor-1-CXC chemokine receptor 4 interactions play a central role in CD4+ T cell accumulation in rheumatoid arthritis synovium. *J. Immunol.* 165:6590–6598.
42. Förster, R., T. Emrich, E. Kremmer, and M. Lipp. 1994. Expression of the G-protein-coupled receptor BLR1 defines mature, recirculating B cells and a subset of T-helper memory cells. *Blood.* 84:830–840.
43. Ansel, K.M., L.J. McHeyzer-Williams, V.N. Ngo, M.G. McHeyzer-Williams, and J.G. Cyster. 1999. In vivo activated CD4 T cells up-regulate CXC chemokine receptor 5 and reprogram their response to lymphoid chemokines. *J. Exp. Med.* 190:1123–1134.
44. Penna, G., S. Sozzani, and L. Adorini. 2001. Cutting edge: selective usage of chemokine receptors by plasmacytoid dendritic cells. *J. Immunol.* 167:1862–1866.
45. Cinamon, G., V. Shinder, and R. Alon. 2001. Shear forces promote lymphocyte migration across vascular endothelium bearing apical chemokines. *Nat. Immunol.* 2:515–522.
46. Hjelmstrom, P. 2001. Lymphoid neogenesis: de novo formation of lymphoid tissue in chronic inflammation through expression of homing chemokines. *J. Leukoc. Biol.* 69:331–339.